

Numerical Heat Transfer, Part A: Applications

An International Journal of Computation and Methodology

ISSN: (Print) (Online) Journal homepage: <https://www.tandfonline.com/loi/unht20>

Heat transfer analysis of MHD Casson nanofluid flow over a nonlinear stretching sheet in the presence of nonuniform heat source

Battena Triveni, Munagala Venkata Subba Rao, Kotha Gangadhar & Ali J. Chamkha

To cite this article: Battena Triveni, Munagala Venkata Subba Rao, Kotha Gangadhar & Ali J. Chamkha (2023): Heat transfer analysis of MHD Casson nanofluid flow over a nonlinear stretching sheet in the presence of nonuniform heat source, Numerical Heat Transfer, Part A: Applications, DOI: [10.1080/10407782.2023.2219831](https://doi.org/10.1080/10407782.2023.2219831)

To link to this article: <https://doi.org/10.1080/10407782.2023.2219831>



Published online: 18 Jun 2023.



Submit your article to this journal [↗](#)



Article views: 51





View related articles [↗](#)



View Crossmark data [↗](#)



Heat transfer analysis of MHD Casson nanofluid flow over a nonlinear stretching sheet in the presence of nonuniform heat source

Battena Triveni^a, Munagala Venkata Subba Rao^a , Kotha Gangadhar^b , and Ali J. Chamkha^c

^aDepartment of Mathematics, School of Applied Science and Humanities, Vignan's Foundation for Science, Technology and Research, Vadlamudi, Andhra Pradesh, India; ^bDepartment of Mathematics, Acharya Nagarjuna University Campus, Ongole, Andhra Pradesh, India; ^cMechanical Engineering, Faculty of Engineering, Kuwait College of Science and Technology, Doha

ABSTRACT

This study examines how a chemical reaction and a nonuniform heat source effect the flow of an MHD Casson nanofluid over a nonlinear stretching sheet. By incorporating viscous dissipation, the energy equation is strengthened. Brownian diffusion, thermophoresis diffusion effects are taken place. By using the necessary similarity transformations, the governing equations for the current flow are converted into a nonlinear system. The RKF technique yields a numerical solution along with a shooting technique for the condensed system. Thereafter, to better understand the physical interpretation of flow and heat transfer, the flow-controlling parameters are shown graphically and in tabular form in the current work. Based on the present study's numerical results, a fair connection is found between this analysis and previous studies. Some of the observations are velocity profile is decreased for the effects of magnetics and stretching parameter variations and Eckert number plays a great role in the increase of temperature profile.

ARTICLE HISTORY

Received 28 February 2023
Revised 13 April 2023
Accepted 22 May 2023

KEYWORDS

Casson nanofluid; chemical reaction; MHD; nonuniform heat source and RKF method; viscous dissipation

1. Introduction

For boundary-driven flows, stretching is one of the most crucial mechanisms. Crane [1] analyzed a precise analytical solution very first to linear stretching on a flat plate. Numerous theoretical and numerical investigations with applications in the engineering and polymer industries have since been carried out. Later on, a numerous studies are carried out to extend this linear stretching to nonlinear as well as exponential stretching velocities for the tubes as well as plane surfaces in both types of fluids Newtonian and Non-Newtonian [2–11]. Researching the two-dimensional boundary layer flow across a nonlinear stretching surface to evaluate the relevance of heat and mass transfer is highly vital and significant since it has so many real-world applications. Aerodynamic extrusion of plastic sheets, extrusion of a polymer sheet from a dye, and condensation of metallic plates in a cooling bath are all practical applications for studying viscous flow over a stretched sheet. These sheets are made by releasing melt through a slit, stretching it till the desired thickness is obtained, and then cutting it into desired shapes. The rates of stretching, cooling, and stretching itself all have a significant impact on the desirable qualities of the final product.

CONTACT Munagala Venkata Subba Rao  mail2mvsr@gmail.com  Department of Mathematics, School of Applied Science and Humanities, Vignan's Foundation for Science, Technology and Research, Vadlamudi, Andhra Pradesh, India.

Actually, the value of heat transfer is simply determined by the thermal conductivity qualities of the working fluids, which include water, ethyl glycol, and oil. A new kind of engineering fluid known as nanofluid is created by sparingly adding nanoparticles (such as Cu, Ag, TiO₂, and Al₂O₃) to such fluids to increase their thermal conductivity [12]. Choi *et al.* [13] investigated and developed the theories in great detail with the goal of enhancing anomalous thermal conductivity in nanotube suspensions. A nanoparticle with a diameter generally between 1 and 100 nm would considerably enhance the thermophysical characteristics of a convective fluid when suspended in it. However, the effort to speed up cooling and heating brings about a number of benefits for industrial processes, including energy.

Ibrahim and Shankar [14] studied the heat transfer and MHD boundary layer flow of a nanofluid *via* a permeable stretching sheet under various boundary conditions for velocity, temperature, and solutal slip. According to Kalidas Das' research [15], the values of the slip parameter and the nonlinear stretching parameter for nanoparticles have an increasing association. Convective transport in fluids is discussed in detail way by Buongiorno [16]. The constant flow across expanding sheet has several more applications in addition to non-Newtonian fluids, MHD flows, porous plates, and heat transfer studies [17].

Zaimi *et al.* [18] also utilized the shooting approach to calculate the boundary layer flow and heat transfer of a nanofluid across a nonlinear porous stretched sheet. Singh *et al.* [19] evaluated mass transpiration in a porous stretched sheet-induced nonlinear MHD flow. Nadeem *et al.* [20] conducted research and found that while the concentration profile improved for higher Ec and Pr values, it decreased for higher Nt levels. Jafar *et al.* [21] looked at MHD radiative nanofluid flow caused by a nonlinear stretching sheet in a porous medium. A nonlinear stretching sheet's MHD boundary layer flow and heat transfer were the subjects of computer research by Mabood *et al.* [22]. Gangadhar *et al.* [23] provided detailed observations of the Buoyancy effect on mixed convection boundary layer flow of Casson fluid over a nonlinear stretched sheet.

In a thorough note on flow, heat transfer analysis, and the application of MHD Casson fluid flow over an exponentially stretching curved sheet in the presence of thermal radiation effect, Anantha Kumar *et al.* [24] provided extensive information. In addition, Venkata Ramudu *et al.* [25] have examined the significance of Soret and Dufour's influence on MHD Casson fluid flow past a stretching surface under convective-diffusive conditions. In response to the stretching of a surface with second-order velocity slip, Kumar *et al.* [26] presented their observations on the flow and heat transfer properties of MHD micropolar fluid. Nandeppanavar [27] investigated laminar boundary layer flow and heat transfer from a warm laminar Casson liquid to a melting sheet moving parallel to a melting stream by numerically with the RKF method. Abel and Nandeppanavar [28] resented a remarkable observation of flow and heat transfer characteristics of visco-elastic fluid flow over an impermeable stretching sheet in the presence of thermal radiation and nonuniform heat source. Later, Bejawada and Nandeppanavar [29] studied the effects of thermal radiation on MHD micropolar fluid flow over a vertical moving porous plate for heat transfer characteristics. Malkeson *et al.* [30] study very clearly about the Numerical investigation of steady-state laminar natural convection of power-law fluids in side-cooled trapezoidal enclosures heated from the bottom. Raju *et al.* [31] examined the dual solutions of MHD boundary layer flow *via* an exponentially stretched sheet with a nonuniform heat source/sink.

The study of an electrically conducting nanofluid has piqued the interest of writers [32–39] due to its importance in engineering and technical processes such as plasma research, MHD generators, MHD pumps, nuclear reactors, geothermal energy extraction, and bearings. Numerous research has focused on the characteristics of heat conduction in porous media, as well as the effect of heat generation, thermal radiation, or viscous dissipation on the flow of boundary layers in nanofluids. Examples of applications include the effect of heat and mass transmission in a nanofluid over a stretched sheet on chemical processes, drying, and energy transfer in a wet cooling tower, fruit tree groves, crop damage from freezing, and other uses. Regarding the effects of

chemical reactions with diverse geometries, numerous authors, including Refs. [40–47], revealed their enlightening discoveries.

The physical conditions are usually connected to a sheet that is linearly stretching in the publications listed above. However, the stretching need not always be linear; it could be quadratic, exponential, and power-law. A nonlinearly stretching sheet may be required in certain physical circumstances. It is, therefore, of utmost importance to understand the flow and heat transfer induced by a nonlinearly extending sheet. Moreover, Researchers pay a lot of attention to non-Newtonian fluid flows because of the growing industrial and technical applications. For example, the needed pumping power might be significantly decreased, if non-Newtonian fluid is used as the coolant or in the heat exchangers. As a result, a fundamental understanding of the flow field of non-Newtonian fluids in a boundary layer next to a stretching sheet or an extended surface is crucial to understanding fluid dynamics and heat transfer. Being motivated by the possible industrial applications and the previous studies regarding the flow and heat transfer of non-Newtonian fluids over the stretching sheet, numerical solution for flow and heat transfer of a laminar boundary layer flow MHD Casson nanofluid over a nonlinear stretching sheet with combined effects of nonuniform heat source and viscous dissipation is presented in this study. Using similarity solutions, the governing equations are transformed into a system of ordinary differential equations, and the RKF method is then applied to numerically determine the solutions. Then, all the numerical data is displayed in figures and tables for easier comprehension of the physical interpretation of the current inquiry. There is a logical correlation between the current study and past investigations.

2. Mathematical formulation

In a steady MHD boundary layer in two dimensions, imagine the flow of a viscous, electrically conducting, and incompressible nanofluid over a nonlinear stretching sheet. For this study, stretching sheet velocity is $u_w(x) = ax^n$ (here, $a > 0$ is called the constant acceleration parameter and n is called the nonlinear stretching parameter). The y -axis represents the surface coordinate, while the x -axis tracks the nonlinear stretching sheet as shown in Figure A. Due to the assumption that the Reynolds number is low, the fluid that conducts electricity when subjected to a magnetic field is ignored. Assume that the nanoparticle fraction C and stretching surface temperature T have constant values of T_w and C_w , respectively. T_∞ and C_∞ , respectively, stand for the ambient values of T and C that have been reached as y tends to infinity. The nanofluid's thermal physical characteristics are thought to stay constant. For the proposed study external forces and the gradient of the pressure are ignored.

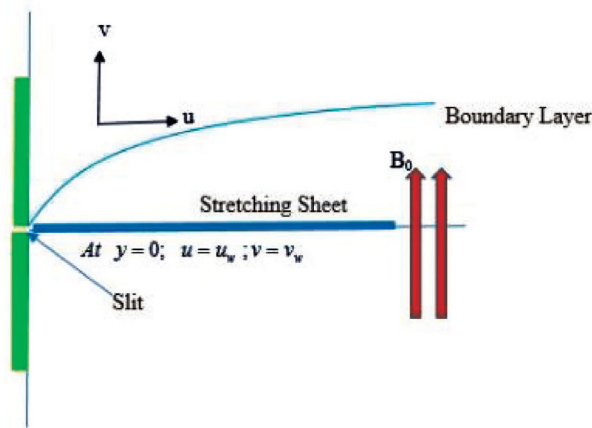


Figure A. Flow diagram for present flow.

The rheological equation of state for an isotropic, incompressible flow of Casson fluid is shown in the following equation [48, 49]:

$$\tau_{ij} = \begin{cases} 2 \left(\mu_B + \frac{P_y}{\sqrt{2\pi}} \right) e_{ij}, & \pi > \pi_c \\ 2 \left(\mu_B + \frac{P_y}{\sqrt{2\pi_c}} \right) e_{ij}, & \pi < \pi_c \end{cases} \quad (1)$$

where, $\pi = e_{ij}e_{ij}$ and e_{ij} represents the (i, j) th component of the deformation rate, π is the product of the component of the deformation rate with itself, indicates fluid yield stress, π indicates a product of the component's rate of deformation with itself, and π_c is the critical value of this product based on the non-Newtonian model, μ_B is the plastic dynamic viscosity of the non-Newtonian fluid and P_y is the yield stress of the fluid.

Here, are the formulae for the alleged flow governing models:

$$\frac{\partial u}{\partial x} + \frac{\partial v}{\partial y} = 0 \quad (2)$$

$$u \frac{\partial u}{\partial x} + v \frac{\partial v}{\partial y} = \nu \left(1 + \frac{1}{\beta} \right) \frac{\partial^2 u}{\partial y^2} - \sigma \frac{B^2}{\rho_f} u \quad (3)$$

$$u \frac{\partial T}{\partial x} + v \frac{\partial T}{\partial y} = \alpha \frac{\partial^2 T}{\partial y^2} + \tau \left[D_B \frac{\partial C}{\partial y} \frac{\partial T}{\partial y} + \frac{D_T}{T_\infty} \left(\frac{\partial T}{\partial y} \right)^2 \right] + \frac{q'''}{(\rho c)_f} + \frac{\nu}{c_p} \left(\frac{\partial u}{\partial y} \right)^2 \quad (4)$$

$$u \frac{\partial C}{\partial x} + v \frac{\partial C}{\partial y} = D_B \frac{\partial^2 C}{\partial y^2} + \frac{D_T}{T_\infty} \left(\frac{\partial^2 T}{\partial y^2} \right) - K(C - C_\infty) \quad (5)$$

The following equation shows the equation for the boundary conditions for this study.

$$\begin{aligned} \text{At } y = 0; \quad u = u_w; \quad v = v_w; \quad T = T_w; \quad C = C_w \\ \text{At } y \rightarrow \infty; \quad u \rightarrow 0; \quad T \rightarrow T_\infty; \quad C \rightarrow C_\infty \end{aligned} \quad (6)$$

where u and v are, respectively, x - and y -axis velocity components. $D_B, D_T, \alpha, \nu, \rho, c, (\rho c)_p, (\rho c)_f$ are defined as in order coefficient of Brownian diffusion, thermophoresis diffusion, fluid thermal diffusivity, kinematic viscosity of the fluid, fluid mass density, specific heat, effective heat capacity, heat capacity. Moreover, variable magnetic field $B(x)$ is thought by numerous writers to have the form $B(x) = B_0 x^{\frac{n-1}{2}}$.

The following equation shows the equation for the nonuniform heat source/sink (q'''):

$$q''' = \left(\frac{k u_w(x)}{xv} \right) [A^*(T_w - T_\infty) f' + B^*(T - T_\infty)] \quad (7)$$

For this study, it is known that k represents thermal conductivity, and A^* and B^* represent the space-dependent and temperature-dependent heat generation/absorption parameters. Further, if these two A^* and B^* are positive, then, it shows an interval heat source nature and if these two are negative, then, it shows that internal heat sink nature.

The following equation shows the similarity transformations there are defined for this study:

$$\begin{aligned}\eta &= y\sqrt{\frac{a(n+1)}{2v}}x^{(n+1)/2}u = ax^n f'(\eta) \\ v &= -\sqrt{\frac{av(n+1)}{2}}x^{(n-1)/2}\left[f(\eta) + \frac{n-1}{n+1}\eta f'(\eta)\right] \\ \phi(\eta) &= \frac{c-c_\infty}{c_w-c_\infty} \quad \theta(\eta) = \frac{T-T_\infty}{T_w-T_\infty}\end{aligned}\quad (8)$$

here, ψ satisfies the C-R equations and which is called the stream function, moreover, it is defined as $u = \frac{\partial\psi}{\partial y}$, $v = -\frac{\partial\psi}{\partial x}$ and temperature, stream function, and concentration functions are indicated θ , $f(\eta)$, and ϕ in order, all these are dimensionless and η is similarity variable.

After all substitutions Eqs. (2)–(4) are as reduced to:

$$\left(1 + \frac{1}{\beta}\right)f''' + ff'' - \frac{2n}{n+1}(f')^2 - Mf' = 0 \quad (9)$$

$$\frac{1}{Pr}\theta'' + \theta'f + Nb\theta'\phi' + Nt(\theta')^2 + \frac{1}{Pr}\left(\frac{2}{n+1}A^*f' + \frac{2}{n+1}B^*\theta\right) + Ecf''^2 = 0 \quad (10)$$

$$\phi'' + Le(f\phi') + \frac{Nt}{Nb}\theta'' - R.Le.\phi = 0 \quad (11)$$

Similarly relevant boundary conditions are changes as

$$\begin{aligned}f'(0) &= 1, \quad f(0) = S, \quad \theta(0) = 1, \quad \phi(0) = 1, \\ f'(\infty) &\rightarrow 0, \quad \theta(\infty) \rightarrow 0, \quad \phi(\infty) \rightarrow 0\end{aligned}\quad (12)$$

here

$$\begin{aligned}M &= \frac{2\sigma B_0^2}{\rho a(n+1)}, \quad Pr = \frac{\nu}{\alpha}, \quad S = \frac{\nu_0}{\sqrt{av}}, \\ Nb &= \frac{\tau D_B(C_w - C_\infty)}{\nu}, \quad Nt = \frac{\tau D_T(T_w - T_\infty)}{T_\infty \nu}, \\ Le &= \frac{\nu}{D_B}, \quad R = \frac{2k_0\nu}{(n+1)a}, \quad \nu = \frac{k}{(\rho c)_f}, \quad Ec = \frac{u_w^2}{c_p(T_w - T_\infty)}.\end{aligned}$$

Formulas for magnetic parameters, Prandtl numbers, suction, Brownian motion, thermophoresis, Lewis numbers, chemical properties, and Eckert numbers are listed in that sequence. Additionally, regional skin friction formulae, regional Sherwood number, and regional Nusselt number are

$$C_{fx} = \frac{\mu_f}{\rho u_w^2} \left(\frac{\partial u}{\partial y}\right)_{y=0}, \quad Nu_x = \frac{xq_w}{k(T_w - T_\infty)}, \quad Sh_x = \frac{xq_m}{D_B(C_w - C_\infty)} \quad (13)$$

where k denotes nanofluid thermal conductivity and q_w , q_m denotes surface heat and mass fluxes in that order and is written as

$$q_w = -\left[\frac{\partial T}{\partial y}\right]_{y=0}, \quad q_m = -D_B\left[\frac{\partial C}{\partial y}\right]_{y=0} \quad (14)$$

After all substitutions, Eqs. (13) and (14) through Eq. (7) becomes

$$Re_x^{1/2}C_{fx} = \left(1 + \frac{1}{\beta}\right)\sqrt{\frac{n+1}{2}}f''(0)$$

$$Re_x^{-1/2} Nu_x = -\sqrt{\frac{n+1}{2}} \theta'(0) \quad (15)$$

$$Re_x^{-1/2} Sh_x = -\sqrt{\frac{n+1}{2}} \phi'(0)$$

Now, $Re_x = u_w x / \nu$ indicates the Reynolds number and its formulae

3. Solution of the problem

To solve the transformed Eqs. (9)–(11) numerically with the help of suitable boundary conditions Eq. (12) R–K–Fehlberg technique along with shooting method is implemented. By means of different types of assumptions, the nonlinear system is reduced to a first-order system to implement the proposed method on reduced system of the first ODEs. They are

$$y_1 = f, y_2 = f', y_3 = f'', y_4 = \theta, y_5 = \theta', y_6 = \phi, y_7 = \phi' \quad (16)$$

The resulting differential equations are given as:

$$y_1' = y_2 \quad (17)$$

$$y_2' = y_3 \quad (18)$$

$$y_3' = \frac{\beta}{1+\beta} \left(\frac{2n}{n+1} y_2^2 + M y_2 - y_1 y_3 \right) \quad (19)$$

$$y_4' = y_5 \quad (20)$$

$$y_5' = -Pr \left(y_1 y_5 + N b y_5 y_7 + N t y_5^2 + \frac{1}{Pr} \left(\frac{2}{n+1} A * y_2 + \frac{2}{n+1} B * y_4 \right) + E c y_5^2 \right) \quad (21)$$

$$y_6' = y_7 \quad (22)$$

$$y_7' = -Le y_1 y_7 - \frac{Nt}{Nb} y_5' + R Le y_6 \quad (23)$$

Corresponding boundary conditions are:

$$\left. \begin{aligned} y_1(0) = S, y_2(0) = 1, y_3(0) = a_1, y_4(0) = 1, y_5(0) = a_2, y_6(0) = 1, y_7(0) = a_3, \\ y_2(\infty) \rightarrow 0, y_4(\infty) \rightarrow 0, y_6(\infty) \rightarrow 0. \end{aligned} \right\} \quad (24)$$

Above reduced system is solved numerically with R–K–Fehlberg by considering suitable values to $a_1, a_2,$ and a_3 . The values of $a_1, a_2,$ and a_3 are chosen by shooting method such that $y_2(\infty) \rightarrow 0, y_4(\infty) \rightarrow 0, y_6(\infty) \rightarrow 0$ are fulfilled. The whole process repeated until they reach the required accuracy and do not impact the solution further increments, the number of steps and size of the starting mesh points are changed with the numerical value of η_∞ . This value is chosen as 6. There is a respectable connection between the results. The Runge–Kutta–Fehlberg method's benefit is based on error control and adjusting the time step to keep the error within a predetermined range. Based on the numerical obtained it can be concluded that the current method performs better in terms of computational speed and offers a more accurate answer when compared to some other existing methods.

3.1. Validation of results and method

To validate the strategy and contrast the current study's findings with those, results from the recommended numerical approach are compared with results from earlier studies that are available

Table 1. Comparison of Nusselt number $[-\theta'(0)]$ when $Nb = Nt = M = S = R = A^* = B^* = Le = Ec = \beta = 0$ and $n = 1$.

Pr	Khan and Pop [50]	Srinvasulu and Shankar [51]	Present results
0.07	0.0633	0.0666	0.0661
0.2	0.1691	0.1691	0.1691
0.7	0.4539	0.4539	0.4539
2	0.9113	0.9115	0.9115
7	1.8954	1.8969	1.8969
20	3.3539	3.3639	3.3413
70	6.4261	6.5447	6.4621

Table 2. Comparison of Nusselt and Sherwood number when $Nb = Nt = 0.5, M = S = R = A^* = B^* = Ec = \beta = 0$ and $Le = 2$.

n	Pr	$-\theta'(0)$			$-\phi'(0)$		
		Rana and Bhargava [52]	Srinvasulu and Shankar [51]	Present results	Rana and Bhargava [52]	Srinvasulu and Shankar [51]	Present results
0.2	0.7	0.3299	0.3252	0.3295	0.8132	0.8058	0.8134
0.3		0.3261	0.3216	0.3262	0.7965	0.7985	0.8067
3		0.3059	0.298	0.3078	0.763	0.7508	0.7682
10		0.3002	0.2922	0.3028	0.7524	0.735	0.7579
20		0.2825	0.2896	0.3016	1.4548	0.7336	0.7553
0.2	2	0.3999	0.3989	0.3987	0.8048	0.8065	0.8059
0.3		0.393	0.3961	0.3959	0.7826	0.7975	0.7970
3		0.3786	0.3777	0.3772	0.7379	0.7389	0.7397
10		0.3739	0.3731	0.3725	0.7238	0.7144	0.7258
20		0.3726	0.371	0.3713	0.7201	0.7178	0.7222
0.2	7	0.2248	0.2214	0.2223	1.0114	1.0156	1.0138
0.3		0.2261	0.222	0.2229	0.9808	1.0033	1.0015
3		0.2288	0.2258	0.2266	0.9185	0.9222	0.9204
10		0.2297	0.2267	0.2274	0.8985	0.9021	0.9005
20		0.2299	0.227	0.2276	0.8933	0.893	0.8953

in the literature for specific situations. All these outcomes are shown in Tables 1 and 2 in order. Now coming to in detail, Nusselt number $-\theta'(0)$ values are recorded and noted in Table 1 by changing the Pr values, moreover by assuming $Nb = 0, Nt = 0, M = 0, R = 0, Le = 0, Ec = 0, S = 0, \beta = 0, A^* = 0, B^* = 0$, and $n = 1$. These results are then compared to the literature [50, 51]. There is a respectable connection between the results. Table 2 provides details regarding the numerical values of $-\theta'(0)$ and $-\phi'(0)$ by changing the n and Pr values and by assuming $Nb = 0.5, Nt = 0.5, M = 0, R = 0, Le = 2, Ec = 0, S = 0, \beta = 0, A^* = 0, B^* = 0$. These results are then compared to the literature [51, 52]. There is a respectable connection between the results.

4. Results and discussion

In this section, the obtained numerical findings are presented in figures and tables to aid in understanding the physical interpretation of the current situation. The impact of the magnetic parameter M on the temperature profile and velocity profile is depicted in Figures 1 and 2. The velocity profile declines with rising magnetic parameter M values. The Lorentz force is to blame. The flow is obstructed by an opposing force. Typically, the Lorentz force causes the fluid in the boundary layer to flow more slowly as shown in Figure 1. This is consistent with the results of Ref. [53]. And temperature profile rises by rising magnetic parameter M values, as displayed in the Figure 2. Reason behind is that the Lorentz force will cause the flow to generate some heat energy. As a result, when M increases, the thermal field and its layer become stronger. This observation is in line with earlier studies of various configurations [54]. In Figures 3 and 4, the impacts of the Casson fluid parameter are displayed for velocity profile and temperature profile. The temperature profile increased as Casson fluid parameter increased, but in case of velocity

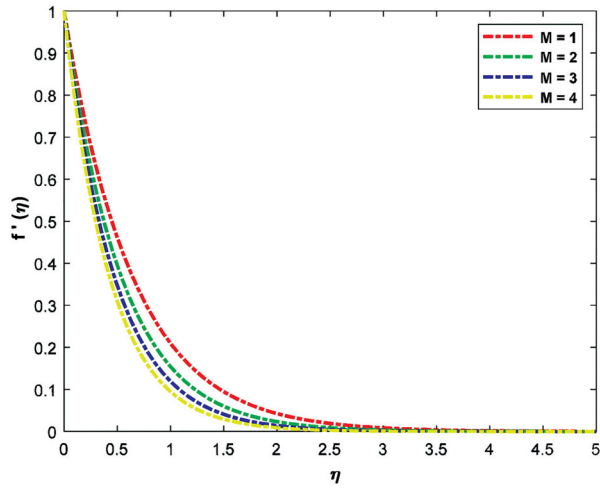


Figure 1. Velocity profile graph for various values of M .

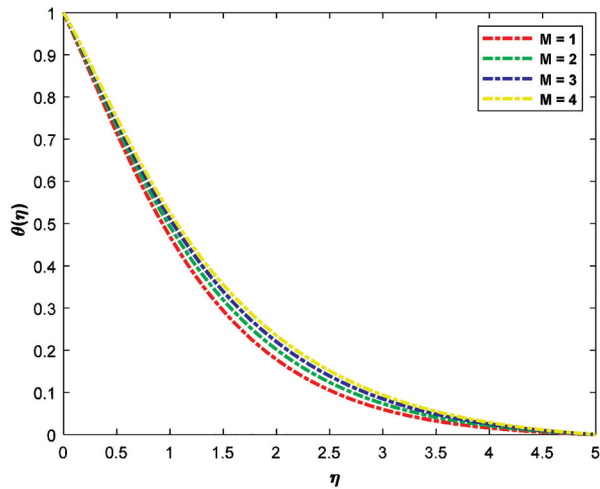


Figure 2. Temperature profile graph for various values of M .

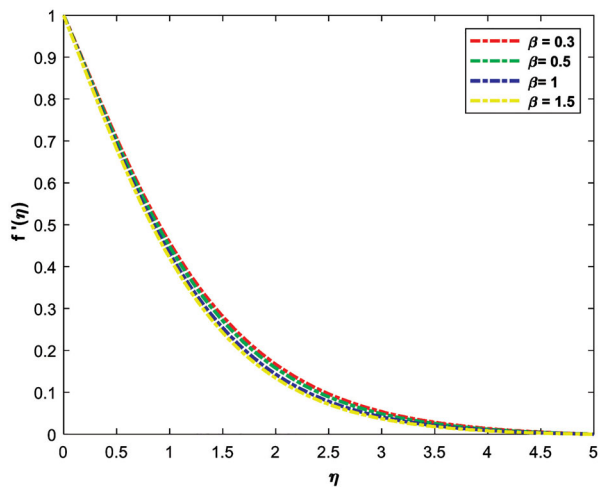


Figure 3. Velocity profile graph for various values of β .

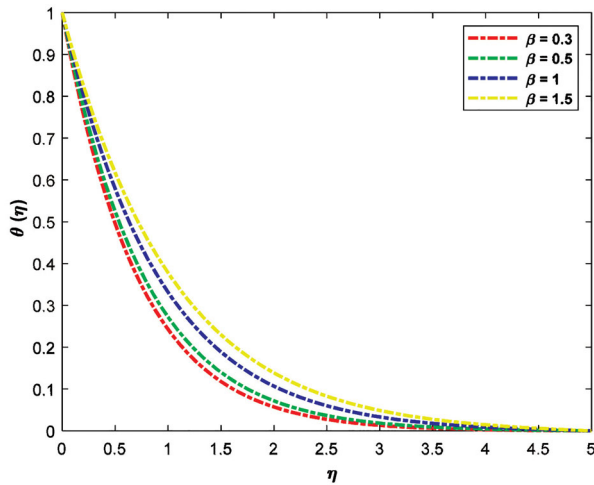


Figure 4. Temperature profile graph for various values of β .

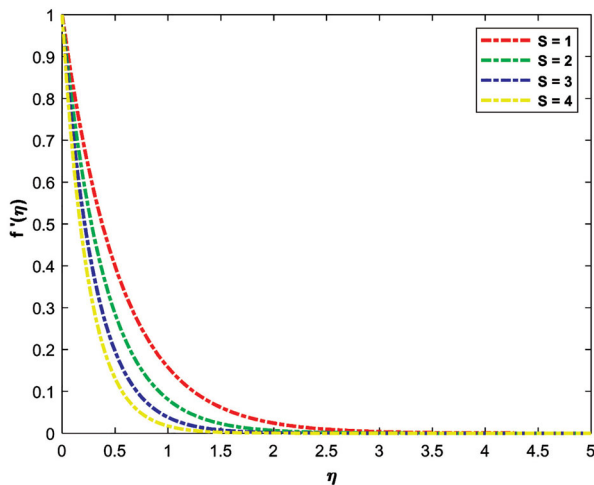


Figure 5. Velocity profile graph for various values of S .

profile reverse trend is noted for the same parametric values. These results unambiguously show that flow separation in the case of a non-Newtonian Casson fluid may be regulated by raising the Casson fluid parameter value. This observation is in line with earlier studies of various configurations [55]. Figures 5–7 show how the suction parameter S influences dimensionless temperature, dimensionless velocity, and the volume fraction of nanoparticles in the boundary layer as S rises. Because of the wall suction, the fluid is drawn closer to the sheet, narrowing the thermal, thermal-nano particle, and momentum boundary layers. These characteristics cause a decrease in the nanoparticles' velocity, temperature, and volume fraction. For nonlinearly stretched sheets, the temperature drops as the Prandtl number rises. The thickness of the thermal boundary layer decreases as the Prandtl number rises. The relative thickening of the momentum and thermal boundary layers in heat transfer issues is governed by the Prandtl number. Because heat diffuses more quickly at low Prandtl numbers than at high velocities, the thermal boundary layer is substantially thicker than the momentum boundary layer for liquid metals. Heat can spread from the sheet more quickly than it can with higher Pr fluids because fluids with lower Prandtl values have higher thermal conductivities. As a result, using the Prandtl value will speed up cooling.

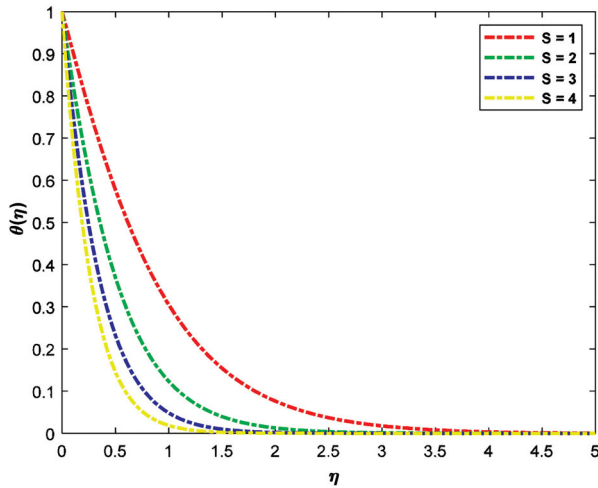


Figure 6. Temperature profile graph for various values of S .

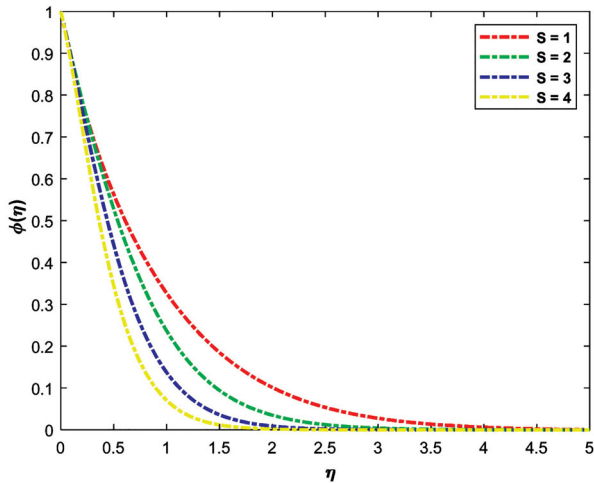


Figure 7. Concentration profile graph for various values of S .

Moreover, as seen in Figure 8, the thermal boundary layer thickness decreases as the Prandtl number rises. This is consistent with the results of Refs. [56, 57]

Figure 9 depicts how the temperature profile is impacted by the space dependent parameter A^* . As the A^* value increases, so does the temperature profile. This is to be estimated as the boundary layer produces energy due to the existence of heat source A^* . The fluid's temperature rises as a result of this. Figures 10 and 11 indicate, respectively, how temperature-dependent parameter B^* impacts temperature and concentration profile. In contrast to Figure 11, which shows the concentration profile for rising values of the temperature-dependent parameter B^* , Figure 10 shows the temperature profile for increasing values of the dependent parameter B^* . As seen in Figures 12 and 13, the thermophoresis parameter Nt has an impact on the temperature and concentration curves. As Nt grew, so did the temperature and the concentration. This is a result of the force known as thermophoresis, which is a quick flow away from the stretched surface. The temperature of the boundary layer rises as Nt rises as more hot fluid is transported away from the surface. The effect of the Brownian motion parameter K on the temperature and concentration profiles of nanofluids over the boundary layer area is seen in Figures 14 and 15. As the

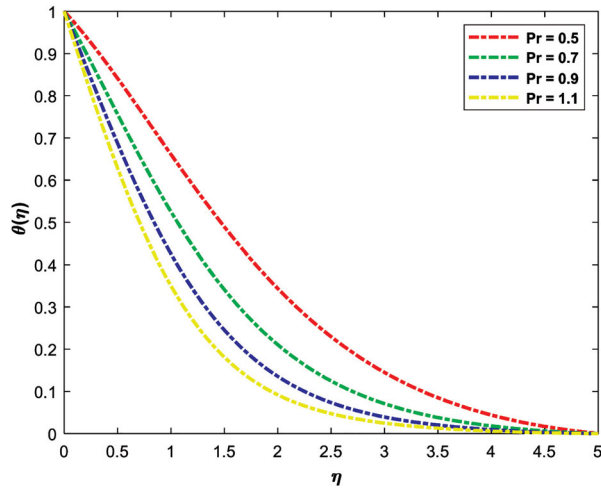


Figure 8. Temperature profile graph for various values of Pr .

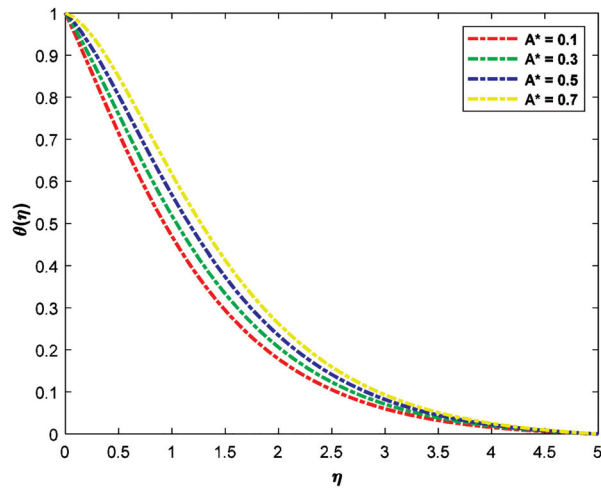


Figure 9. Temperature profile graph for various values of A^* .

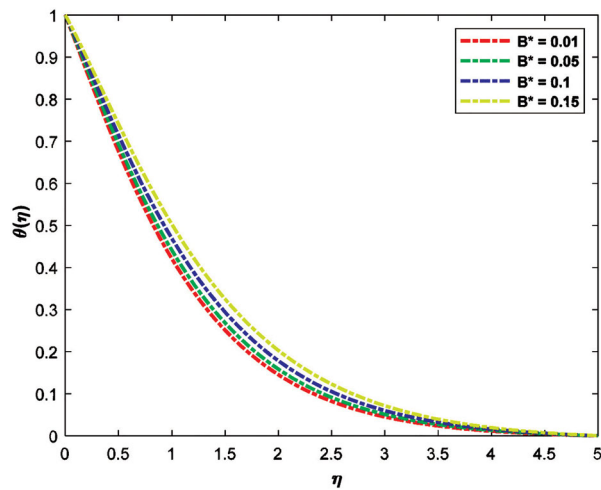


Figure 10. Temperature profile graph for various values of B^* .

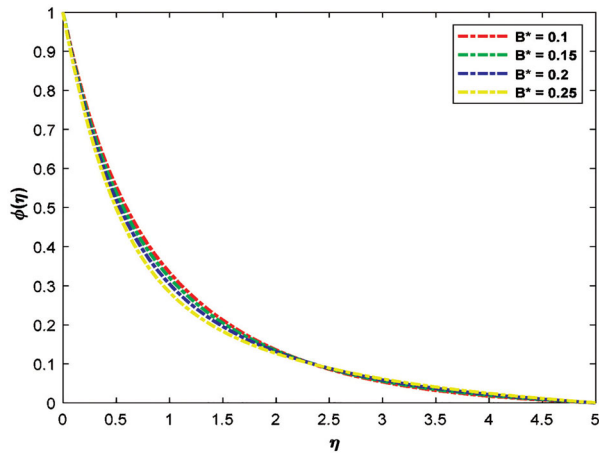


Figure 11. Concentration profile graph for various values of B^* .

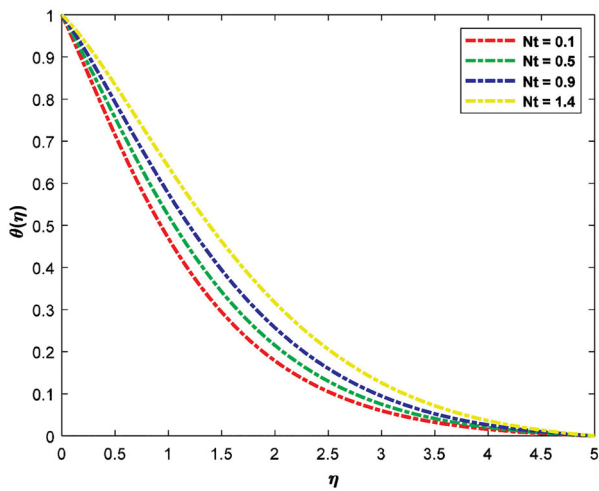


Figure 12. Temperature profile graph for various values of Nt .

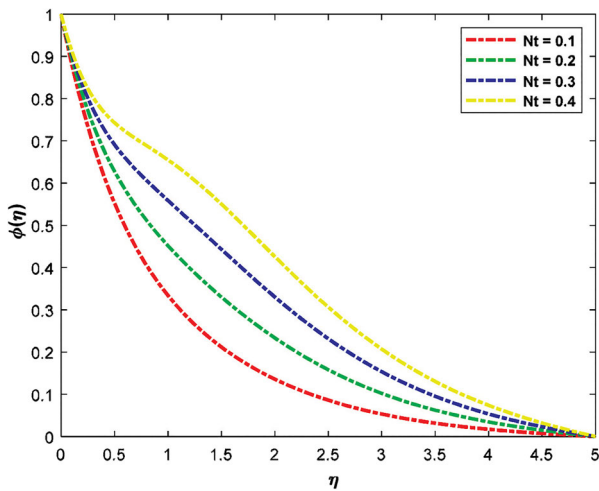


Figure 13. Concentration profile graph for various values of Nt .

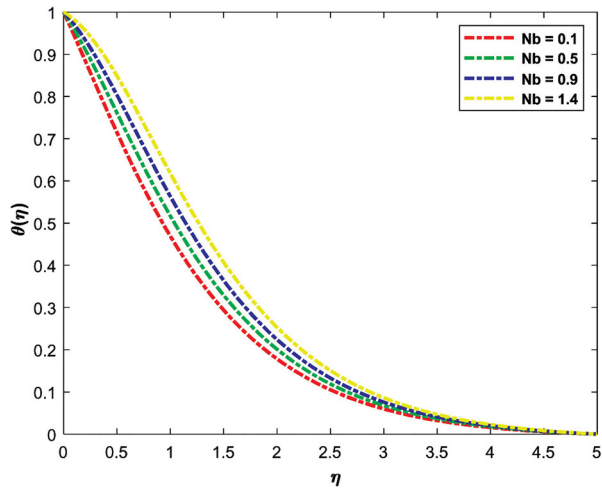


Figure 14. Temperature profile graph for various values of Nb .

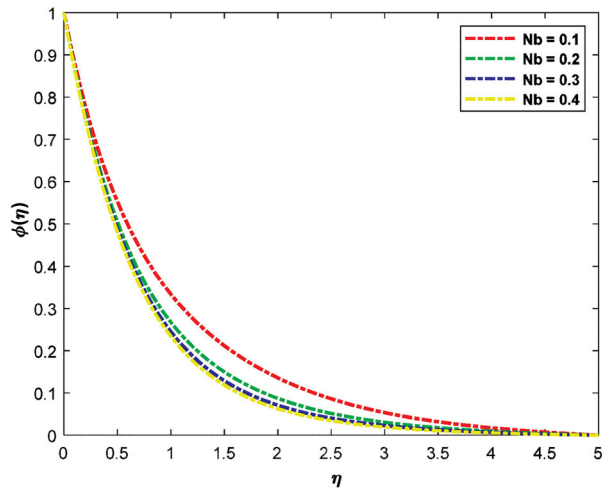


Figure 15. Concentration profile graph for various values of Nb .

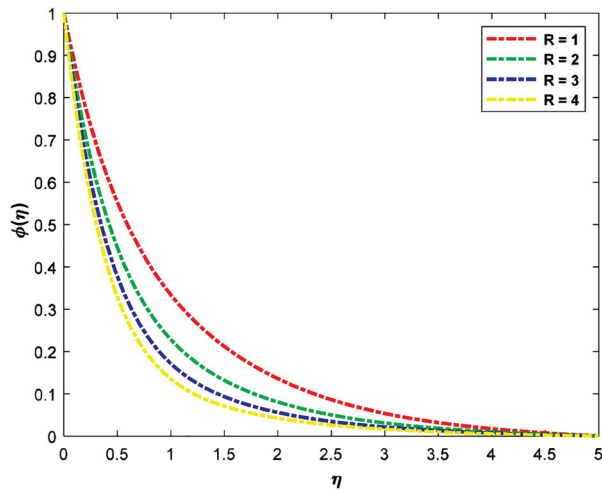


Figure 16. Concentration profile graph for various values of R .

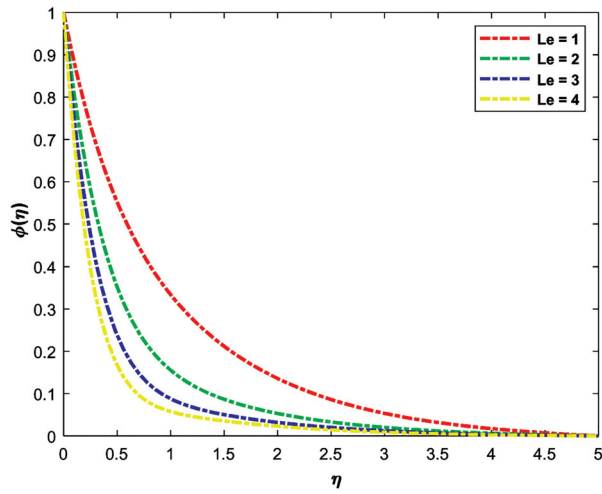


Figure 17. Concentration profile graph for various values of Le .

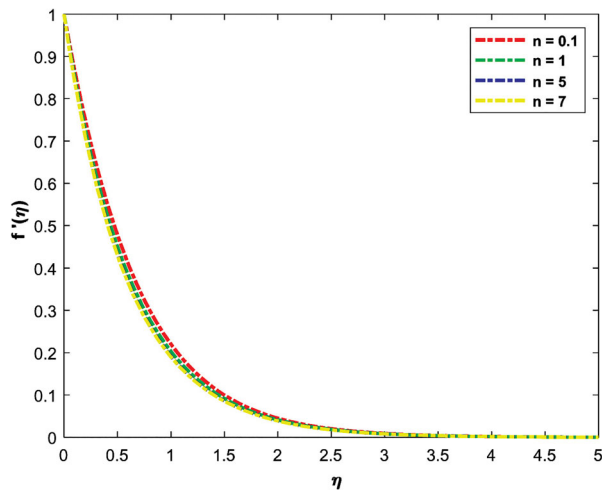


Figure 18. Velocity profile graph for various values of n .

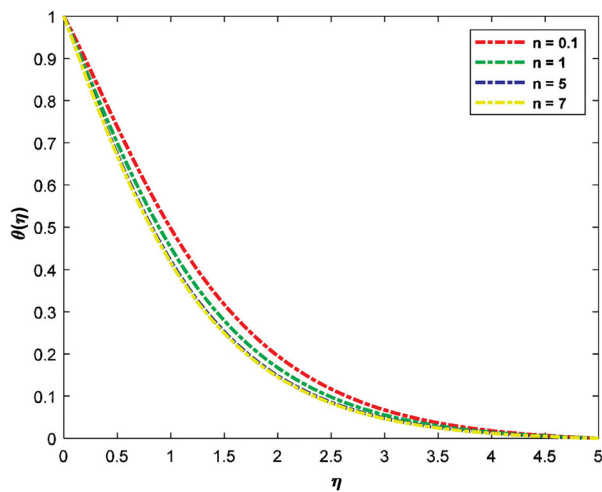


Figure 19. Temperature profile graph for various values of n .

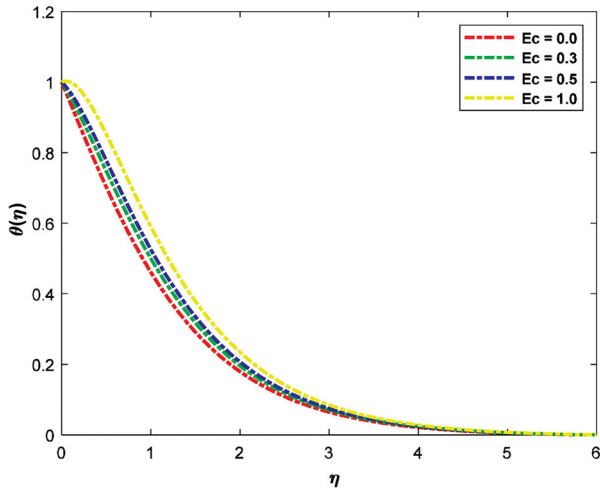


Figure 20. Temperature profile graph for various values of Ec .

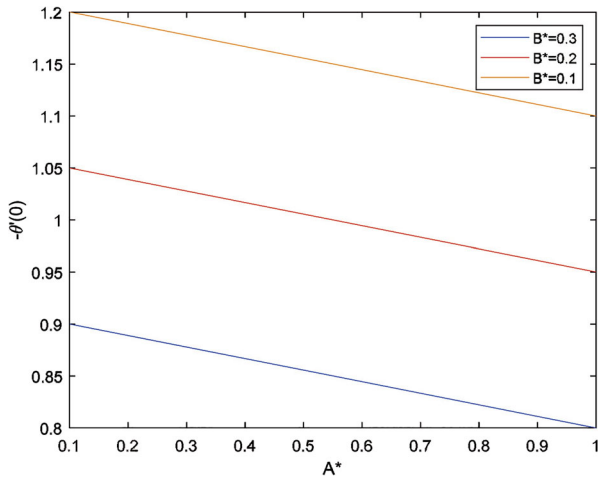


Figure 21. Effect of B^* on Nusselt number if $M = Le = Pr = R = S = 1, Nb = Nt = 0.1, n = 0.5$.

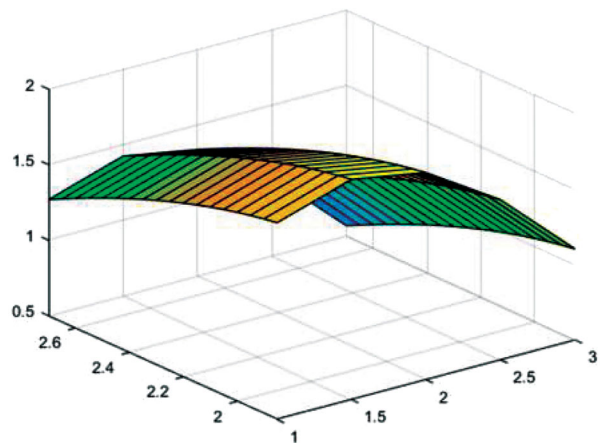


Figure 22. Effect of n on Skin friction when $Le = Pr = R = S = 1$ and $A^* = B^* = Nb = Nt = 0.1$.

Table 3. Skin friction, the Nusselt number, and the Sherwood number in numerical form for various parameter values.

Pr	Nb	Nt	A^*	B^*	Le	R	M	S	n	Skin friction	Nusselt number	Sherwood number
1	0.1	0.1	0.1	0.1	1	1	1	1	0.5	1.813497	0.951126	1.250195
2										1.813497	1.859497	0.445266
1	0.2									1.813497	0.887259	1.551095
	0.3									1.813497	0.826450	1.650397
	0.1	0.2								1.813497	0.911258	0.776087
		0.3								1.813497	0.872856	0.366959
			0.2							1.813497	0.884433	1.399676
			0.3							1.813497	0.817692	1.369200
			0.1	0.2						1.813497	0.842442	1.343864
				0.3						1.813497	0.710800	1.455760
					2					1.813497	0.935584	2.542173
					3					1.813497	0.928489	3.715679
						2				1.813497	0.944032	1.723703
						3				1.813497	0.939703	2.081534
							2			2.113251	0.918565	1.264480
							3			2.367060	0.891891	1.277559
								2		2.483141	1.802715	1.143563
								3		3.238909	2.672041	1.077413
									1	1.877501	0.987463	1.216260
									1.5	1.914807	1.008680	1.196422

Brownian motion parameter is increased, the temperature in the boundary layer rises. As Nb increases, the temperature rises as a result of the growing kinetic energy of moving nanoparticles. A significant exception is the volume fraction profile of nanoparticles. Figure 16 depicts the variation of the chemical parameter R along the concentration profile. The concentration profile declines when the parameters of a chemical process are raised. In Figure 17, it is possible to see how the Lewis number Le affected the concentration profile. As the volume fraction of nanoparticles varies across the stretched sheet, the thickness of the volume fraction boundary layer decreases. The temperature and velocity profiles of nanofluids are shown in Figures 18 and 19 as a function of the nonlinear stretching parameter n . The temperature and velocity of the Nano fluid decrease when the value of n is increased due to nonlinear stretching. The temperature curves for various Eckert number Ec values are shown in Figure 20. The temperature of the boundary layer rises as the Eckert number Ec grows. The reason behind this that increasing the Eckert number produces more heat, which is then stored in the fluid due to strong forces of friction between the fluid's particles. As a result, temperature distribution becomes more intense. This observation is in line with earlier studies of various configurations [58]. The impact of A^* and B^* on the Nusselt number is seen in Figure 21. The rate of heat transport increases as B^* values decrease.

The skin friction coefficient is influenced by the magnetic and nonlinear stretching components, as seen in Figure 22. The rate of velocity increases when n is increased. Table 3 shows the variation of the Sherwood number, Nusselt number, and Skin friction coefficient for various values of the parameters M , Pr , Le , Nb , Nt , S , R , A^* , B^* , and n .

5. Conclusions

The flow of an MHD Casson nanofluid over a nonlinear stretching sheet in the presence of a nonuniform heat source is investigated computationally to evaluate the effects of viscous dissipation and chemical reaction. The right similarity transformations are used to turn the current flow governing equations into a nonlinear system, which is then numerically solved using the RKF approach along with shooting technique. The physical interpretation of the current study can be explored by graphing the various flow-controlling parameters involved in this analysis, including the Brownian motion parameter, Lewis number, chemical reaction parameter, suction parameter,

nonlinear stretching parameter, Prandtl number, and thermophoresis parameter. For the skin friction, Sherwood number, and Nusslet number data is presented in tabular format. The study's main findings are the following.

1. When magnetic parameter values increased, the velocity profile diminishes, while temperature distribution shows a reverse trend.
2. When Casson fluid parameter values increased, velocity profile diminishes, while temperature distribution shows reverse trend.
3. The temperature distribution grows along with the Eckert number.
4. The profiles of velocity, temperature, and concentration decreased with increasing numerical value of the suction parameter.
5. The nonuniform heat source parameter's values increase as the temperature distribution does, while the concentration profile shows the opposite trend.
6. Increases in Pr value cause the Nusselt number to rise, but increases in Nb , Nt , A^* , B^* , Le , R , M cause the opposite to occur.
7. The Sherwood number rises as Nb , Le , R , and grow while falling when Pr and Nt rise.
8. When M and S increase, skin friction coefficient increases.

ORCID

Munagala Venkata Subba Rao  <http://orcid.org/0000-0002-5188-223X>

Kotha Gangadhar  <http://orcid.org/0000-0002-0264-2512>

References

- [1] L. J. Crane, "Flow past a stretching plate," *J. Appl. Math. Phys.*, vol. 21, no. 4, pp. 645–647, Jul. 1970. DOI: [10.1007/BF01587695](https://doi.org/10.1007/BF01587695).
- [2] V. Kumaran and G. Ramanaiah, "A note on the flow over stretching sheet," *Acta Mech.*, vol. 116, no. 1–4, pp. 229–233, Mar. 1996. DOI: [10.1007/BF01171433](https://doi.org/10.1007/BF01171433).
- [3] A. Raptis and C. Perdikis, "Viscous flow over a nonlinear stretching sheet in the presence of a chemical reaction and magnetic field," *Int. J. Nonlinear Mech.*, vol. 41, no. 4, pp. 527–529, May 2006. DOI: [10.1016/j.ijnonlinmec.2005.12.003](https://doi.org/10.1016/j.ijnonlinmec.2005.12.003).
- [4] R. Cortell, "Further results on nonlinearly stretching permeable sheets. Analytic solution for MHD flow and mass transfer," *Math. Probl. Eng.*, vol. 2012, no. 12, pp. 1–18, Dec. 2012. DOI: [10.1155/2012/743130](https://doi.org/10.1155/2012/743130).
- [5] N. A. Kelson, "Note on similarity solutions for viscous flow over an impermeable and non-linearly (quadratic) stretching sheet," *Int. J. Nonlinear Mech.*, vol. 46, no. 8, pp. 1090–1091, Oct. 2011. DOI: [10.1016/j.ijnonlinmec.2011.04.025](https://doi.org/10.1016/j.ijnonlinmec.2011.04.025).
- [6] R. Cortell, "MHD (magneto-hydrodynamic) flow and radiative nonlinear heat transfer of a viscoelastic fluid over a stretching sheet with heat generation/absorption," *Energy*, vol. 74, pp. 896–905, Sept. 2014. DOI: [10.1016/j.energy.2014.07.069](https://doi.org/10.1016/j.energy.2014.07.069).
- [7] M. Abd-El-Aziz, "Viscous dissipation effect on mixed convection flow of a micropolar fluid over an exponentially stretching sheet," *Can. J. Phys.*, vol. 87, no. 4, pp. 359–368, Jun. 2009. DOI: [10.1139/P09-047](https://doi.org/10.1139/P09-047).
- [8] A. Ishak, "MHD boundary layer flow due to an exponentially stretching sheet with radiation effect," *Sains Malaysiana*, vol. 40, no. 4, pp. 391–395, Apr. 2011.
- [9] A. Zeeshan and R. Ellahi, "Series solutions for nonlinear partial differential equations with slip boundary conditions for non-Newtonian MHD fluid in porous space," *Appl. Math. Inf. Sci.*, vol. 7, no. 1, pp. 257–265, Jan. 2013. DOI: [10.12785/amis/070132](https://doi.org/10.12785/amis/070132).
- [10] K. M. Sanni, Q. Hussain, and S. Asghar, "Heat transfer analysis for non-linear boundary driven flow over a curved stretching sheet with a variable magnetic field," *Front. Phys.*, vol. 8, pp. 113, Apr. 2020. DOI: [10.3389/fphy.2020.00113](https://doi.org/10.3389/fphy.2020.00113).
- [11] J. Alinejad and S. Samarbakhsh, "Viscous flow over nonlinearly stretching sheet with effects of viscous dissipation," *J. Appl. Math.*, vol. 2012, pp. 1–10, May 2012. DOI: [10.1155/2012/587834](https://doi.org/10.1155/2012/587834).
- [12] S. U. S. Choi and J. A. Eastman, "Enhancing thermal conductivity of fluids with nanoparticles," Proceedings of the ASME Materials Division: presented at the 1995 ASME International Mechanical Engineering Congress and Exposition, San Francisco, California, November 12–17, 1995.

- [13] S. U. S. Choi, Z. G. Zhang, W. Yu, F. E. Lockwood, and E. A. Grulke, "Anomalous thermal conductivity enhancement in nanotube suspensions," *Appl. Phys. Lett.*, vol. 79, no. 14, pp. 2252–2254, Oct. 2001. DOI: [10.1063/1.1408272](https://doi.org/10.1063/1.1408272).
- [14] W. Ibrahim and B. Shankar, "MHD boundary layer flow and heat transfer of a nanofluid past a permeable stretching sheet with velocity, thermal and solutal slip boundary conditions," *Comput. Fluids*, vol. 75, pp. 1–10, Apr. 2013. DOI: [10.1016/j.compfluid.2013.01.014](https://doi.org/10.1016/j.compfluid.2013.01.014).
- [15] K. Das, "Nano fluid flow over a non-linear permeable stretching sheet with partial slip," *J. Egypt. Math. Soc.*, vol. 23, no. 2, pp. 451–456, Jul. 2015. DOI: [10.1016/j.joems.2014.06.014](https://doi.org/10.1016/j.joems.2014.06.014).
- [16] J. Buongiorno, "Convective transport in nano fluids," *J. Heat Transf.*, vol. 128, no. 3, pp. 240–250, Mar. 2006. DOI: [10.1115/1.2150834](https://doi.org/10.1115/1.2150834).
- [17] S. V. Desale and V. H. Pradhan, "Implicit finite difference solution of boundary layer heat flow over a flat plate," *IOSR-JM.*, vol. 9, no. 3, pp. 16–21, Dec. 2013. DOI: [10.9790/5728-0931621](https://doi.org/10.9790/5728-0931621).
- [18] K. Zaimi, A. Ishak, and I. Pop, "Boundary layer flow and heat transfer over a nonlinearly permeable stretching/shrinking sheet in a nanofluid," *Sci. Rep.*, vol. 4, no. 1, pp. 4404, Mar. 2014. DOI: [10.1038/srep04404](https://doi.org/10.1038/srep04404).
- [19] J. Singh, U. S. Mahabaleshwar, and G. Bognár, "Mass transpiration in nonlinear MHD flow due to porous stretching sheet," *Sci. Rep.*, vol. 9, no. 1, pp. 18484, Dec. 2019. DOI: [10.1038/s41598-019-52597-5](https://doi.org/10.1038/s41598-019-52597-5).
- [20] S. Nadeem *et al.*, "Numerical computations for Buongiorno nano fluid model on the boundary layer flow of viscoelastic fluid towards a nonlinear stretching sheet," *Alex. Eng. J.*, vol. 61, no. 2, pp. 1769–1778, Feb. 2022. DOI: [10.1016/j.aej.2021.11.013](https://doi.org/10.1016/j.aej.2021.11.013).
- [21] A. B. Jafar, S. Shafie, and I. Ullah, "MHD radiative nanofluid flow induced by a nonlinear stretching sheet in a porous medium," *Heliyon.*, vol. 6, no. 6, pp. e04201, Jun. 2020. DOI: [10.1016/j.heliyon.2020.e04201](https://doi.org/10.1016/j.heliyon.2020.e04201).
- [22] F. Mabood, W. A. Khan, and A. I. M. Ismail, "MHD boundary layer flow and heat transfer of nano fluids over a nonlinear stretching sheet: A numerical study," *J. Magn. Magn. Mater.*, vol. 374, pp. 569–576, Jan. 2015. DOI: [10.1016/j.jmmm.2014.09.013](https://doi.org/10.1016/j.jmmm.2014.09.013).
- [23] K. Gangadhar, R. Edukondala Nayak, and M. Venkata Subba Rao, "Buoyancy effect on mixed convection boundary layer flow of Casson fluid over a non-linear stretched sheet using the spectral relaxation method," *Int. J. Ambient Energy*, vol. 43, no. 1, pp. 1994–2002, Feb. 2022. DOI: [10.1080/01430750.2020.1722963](https://doi.org/10.1080/01430750.2020.1722963).
- [24] K. Anantha Kumar, V. Sugunamma, and N. Sandeep, "Effect of thermal radiation on MHD Casson fluid flow over an exponentially stretching curved sheet," *J. Therm. Anal. Calorim.*, vol. 140, no. 5, pp. 2377–2385, Nov. 2020. DOI: [10.1007/s10973-019-08977-0](https://doi.org/10.1007/s10973-019-08977-0).
- [25] A. C. Venkata Ramudu, K. Anantha Kumar, V. Sugunamma, and N. Sandeep, "Impact of Soret and Dufour on MHD Casson fluid flow past a stretching surface with convective–diffusive conditions," *J. Therm. Anal. Calorim.*, vol. 147, no. 3, pp. 2653–2663, Feb. 2022. DOI: [10.1007/s10973-021-10569-w](https://doi.org/10.1007/s10973-021-10569-w).
- [26] K. A. Kumar, V. Sugunamma, N. Sandeep, and M. T. Mustafa, "Simultaneous solutions for first order and second order slips on micropolar fluid flow across a convective surface in the presence of Lorentz force and variable heat source/sink," *Sci. Rep.*, vol. 9, no. 1, pp. 14706, Oct. 2019. DOI: [10.1038/s41598-019-51242-5](https://doi.org/10.1038/s41598-019-51242-5).
- [27] M. M. Nandeppanavar, "Melting heat transfer analysis of non-Newtonian Casson fluid due to moving plate," *EC.*, vol. 35, no. 3, pp. 1301–1313, May 2018. DOI: [10.1108/EC-04-2017-0148](https://doi.org/10.1108/EC-04-2017-0148).
- [28] M. S. Abel and M. M. Nandeppanavar, "Effects of thermal radiation and non-uniform heat source on MHD flow of viscoelastic fluid and heat transfer over a stretching sheet," *Int. J. Appl. Mech. Eng.*, vol. 12, no. 4, pp. 903–918, 2007.
- [29] S. G. Bejawada and M. M. Nandeppanavar, "Effect of thermal radiation on magneto hydrodynamics heat transfer micropolar fluid flow over a vertical moving porous plate," *Exp. Comput. Multiph. Flow*, vol. 5, no. 2, pp. 149–158, Mar. 2023. DOI: [10.1007/s42757-021-0131-5](https://doi.org/10.1007/s42757-021-0131-5).
- [30] S. P. Malkeson, S. Alshaaaili, and N. Chakraborty, "Numerical investigation of steady state laminar natural convection of power-law fluids in side-cooled trapezoidal enclosures heated from the bottom," *Numer. Heat Transf. Part A: Appl.*, vol. 83, no. 7, pp. 770–789, Jan. 2023. DOI: [10.1080/10407782.2022.2157353](https://doi.org/10.1080/10407782.2022.2157353).
- [31] C. S. K. Raju, N. Sandeep, C. Sulochana, and M. Jayachandra Babu, "Dual solutions of MHD boundary layer flow past an exponentially stretching sheet with non-uniform heat source/sink," *JAFM.*, vol. 9, no. 2, pp. 555–563, Feb. 2016. DOI: [10.18869/acadpub.jafm.68.225.24784](https://doi.org/10.18869/acadpub.jafm.68.225.24784).
- [32] W. N. Mutuku, "MHD non-linear boundary layer flow and heat transfer of nanofluids past a permeable moving flat surface with thermal radiation and viscous dissipation," *Univer. J. Fluid Mech.*, vol. 2, pp. 55–68, 2014.
- [33] A. Lazarus Godson, "Nano fluid heat transfer and applications," *J. Therm. Eng.*, vol. 1, no. 2, pp. 113–115, Apr. 2015.
- [34] N. G. Rudraswamy and B. J. Gireesha, "Influence of chemical reaction and thermal radiation on MHD boundary layer flow and heat transfer of a nano fluid over an exponentially stretching sheet," *JAMP.*, vol. 02, no. 02, pp. 24–32, Jan. 2014. DOI: [10.4236/jamp.2014.22004](https://doi.org/10.4236/jamp.2014.22004).

- [35] P. S. Gupta and A. S. Gupta, "Heat and mass transfer on a stretching sheet with suction or blowing," *Can. J. Chem. Eng.*, vol. 55, no. 6, pp. 744–746, Dec. 1977. DOI: [10.1002/cjce.5450550619](https://doi.org/10.1002/cjce.5450550619).
- [36] E. Magyari and B. Keller, "Heat and mass transfer in the boundary layers on an exponentially stretching continuous surface," *J. Phys. D: Appl. Phys.*, vol. 32, no. 5, pp. 577–585, Mar. 1999. DOI: [10.1088/0022-3727/32/5/012](https://doi.org/10.1088/0022-3727/32/5/012).
- [37] N. Sandeep and C. Sulochana, "Dual solutions for unsteady mixed convection flow of MHD micropolar fluid over a stretching/shrinking sheet with non-uniform heat source/sink," *Eng. Sci. Technol. Int. J.*, vol. 18, no. 4, pp. 738–745, Dec. 2015. DOI: [10.1016/j.jestch.2015.05.006](https://doi.org/10.1016/j.jestch.2015.05.006).
- [38] M. G. Reddy, "Influence of magneto hydrodynamic and thermal radiation boundary layer flow of a nano fluid past a stretching sheet," *J. Sci. Res.*, vol. 6, no. 2, pp. 257–272, Apr. 2014. DOI: [10.3329/jsr.v6i2.17233](https://doi.org/10.3329/jsr.v6i2.17233).
- [39] N. S. Yousef, A. M. Megahed, I. N. Ghoneim, M. Elsafi, and E. Fares, "Chemical reaction impact on MHD dissipative Casson-Williamson nanofluid flow over a slippery stretching sheet through porous medium," *Alex. Eng. J.*, vol. 61, no. 12, pp. 10161–10170, Dec. 2022. DOI: [10.1016/j.aej.2022.03.032](https://doi.org/10.1016/j.aej.2022.03.032).
- [40] S. Ahmad, M. Naveed Khan, and S. Nadeem, "Unsteady three dimensional bioconvective flow of Maxwell nanofluid over an exponentially stretching sheet with variable thermal conductivity and chemical reaction," *Int. J. Ambient Energy*, vol. 43, no. 1, pp. 6542–6552, Feb. 2022. DOI: [10.1080/01430750.2022.2029765](https://doi.org/10.1080/01430750.2022.2029765).
- [41] H. Dessie and N. Kishan, "Unsteady MHD flow of heat and mass transfer of nanofluids over stretching sheet with a non-uniform heat/source/sink considering viscous dissipation and chemical reaction," *JERA.*, vol. 14, pp. 1–12, Mar. 2015. DOI: [10.4028/www.scientific.net/JERA.14.1](https://doi.org/10.4028/www.scientific.net/JERA.14.1).
- [42] T. Vijayalaxmi and B. Shankar, "Hydromagnetic flow and heat transfer of Williamson nanofluid over an inclined exponential stretching sheet in the presence of thermal radiation and chemical reaction with slip conditions," *J. Nanofluids*, vol. 5, no. 6, pp. 826–838, Dec. 2016. DOI: [10.1166/jon.2016.1283](https://doi.org/10.1166/jon.2016.1283).
- [43] R. M. Kasmani, S. Sivasankaran, M. Bhuvaneswari, and Z. Siri Kasmani, "Effect of chemical reaction on convective heat transfer of boundary layer flow in nanofluid over a wedge with heat generation/absorption and suction," *JAFM.*, vol. 9, no. 1, pp. 379–388, Dec. 2016. DOI: [10.18869/acadpub.jafm.68.224.24151](https://doi.org/10.18869/acadpub.jafm.68.224.24151).
- [44] S. A. Shehzad, T. Hayat, M. Qasim, and S. Asghar, "Effects of mass transfer on MHD flow of Casson fluid with chemical reaction and suction," *Braz. J. Chem. Eng.*, vol. 30, no. 1, pp. 187–195, Mar. 2013. DOI: [10.1590/S0104-66322013000100020](https://doi.org/10.1590/S0104-66322013000100020).
- [45] B. C. Prasannakumara, B. J. Gireesha, Rama, S. R. Gorla, and M. R. Krishnamurthy, "Effects of chemical reaction and nonlinear thermal radiation on Williamson nanofluid slip flow over a stretching sheet embedded in a porous medium," *J. Aerosp. Eng.*, vol. 29, no. 5, Sept. 2016. DOI: [10.1061/\(ASCE\)AS.1943-5525.0000578](https://doi.org/10.1061/(ASCE)AS.1943-5525.0000578).
- [46] M. R. Krishnamurthy, B. C. Prasanna Kumara, B. J. Gireesha, and G. Rama Subba Reddy, "Effect of chemical reaction on MHD boundary layer flow and melting heat transfer of williamson nano fluid in porous medium," *Eng. Sci. Technol.*, vol. 19, no. 1, pp. 53–61, Mar. 2016. DOI: [10.1016/j.jestch.2015.06.010](https://doi.org/10.1016/j.jestch.2015.06.010).
- [47] S. M. Abo-Dahab, M. A. Abdelhafez, F. Mebarek-Oudina, and S. M. Bilal, "MHD Casson nanofluid flow over nonlinearly heated porous medium in presence of extending surface effect with suction/injection," *Indian J. Phys.*, vol. 95, no. 12, pp. 2703–2717, Jan. 2021. DOI: [10.1007/s12648-020-01923-z](https://doi.org/10.1007/s12648-020-01923-z).
- [48] M. Nakamura and T. Sawada, "Numerical study on the flow of a non-Newtonian fluid through an axisymmetric stenosis," *J. Biomech. Eng.*, vol. 110, no. 2, pp. 137–143, May 1988. DOI: [10.1115/1.3108418](https://doi.org/10.1115/1.3108418).
- [49] S. Mukhopadhyay, I. C. Mondal, and A. J. Chamkha, "Casson fluid flow and heat transfer past a symmetric wedge," *Heat Transf. Asian Res.*, vol. 42, no. 8, pp. 665–675, Jun. 2013. DOI: [10.1002/htj.21065](https://doi.org/10.1002/htj.21065).
- [50] W. A. Khan and I. Pop, "Boundary-layer flow of a nanofluid past a stretching sheet," *Int. J. Heat Mass Transf.*, vol. 53, no. 11–12, pp. 2477–2483, May 2010. DOI: [10.1016/j.ijheatmasstransfer.2010.01.032](https://doi.org/10.1016/j.ijheatmasstransfer.2010.01.032).
- [51] T. Srinvasulu and S. Bandari, "MHD boundary layer flow of nanofluid over a nonlinear stretching sheet with effect of non-uniform heat source and chemical reaction," *J. Nanofluids*, vol. 6, no. 4, pp. 637–646, Aug. 2017. DOI: [10.1166/jon.2017.1362](https://doi.org/10.1166/jon.2017.1362).
- [52] P. Rana and R. Bhargava, "Flow and heat transfer of a nanofluid over a nonlinearly stretching sheet: A numerical study," *Commun. Nonlinear Sci. Numer. Simul.*, vol. 17, no. 1, pp. 212–226, Jan. 2012. DOI: [10.1016/j.cnsns.2011.05.009](https://doi.org/10.1016/j.cnsns.2011.05.009).
- [53] K. Anantha Kumar, V. Sugunamma, and N. Sandeep, "Influence of variable viscosity on 3-D MHD radiative cross nanofluid flow over a biface region," *Waves Random Complex Media*, pp. 1–16, Aug. 2022. DOI: [10.1080/17455030.2022.2104953](https://doi.org/10.1080/17455030.2022.2104953).
- [54] K. Anantha Kumar, V. Sugunamma, and N. Sandeep, "Impact of non-linear radiation on MHD non-aligned stagnation point flow of micropolar fluid over a convective surface," *J. Non-Equilib. Thermodyn.*, vol. 43, no. 4, pp. 327–345, Aug. 2018. DOI: [10.1515/jnet-2018-0022](https://doi.org/10.1515/jnet-2018-0022).
- [55] K. Anantha Kumar, A. C. Venkata Ramudu, V. Sugunamma, and N. Sandeep, "Effect of non-linear thermal radiation on MHD Casson fluid flow past a stretching surface with chemical reaction," *Int. J. Ambient Energy*, vol. 43, no. 1, pp. 8400–8407, Jul. 2022. DOI: [10.1080/01430750.2022.2097947](https://doi.org/10.1080/01430750.2022.2097947).

- [56] K. Anantha Kumar, J. V. Ramana Reddy, V. Sugunamma, and N. Sandeep, "Magneto hydrodynamic Cattaneo-Christov flow past a cone and a wedge with variable heat source/sink," *Alex. Eng. J.*, vol. 57, no. 1, pp. 435–443, Mar. 2018. DOI: [10.1016/j.aej.2016.11.013](https://doi.org/10.1016/j.aej.2016.11.013).
- [57] M. M. Nandeppanavar, M. C. Kemparaju, and S. Shakunthala, "MHD stagnation point slip flow due to a non-linearly moving surface with effect of non-uniform heat source," *Nonlinear Eng.*, vol. 8, no. 1, pp. 270–282, Jul. 2019. DOI: [10.1515/nleng-2017-0109](https://doi.org/10.1515/nleng-2017-0109).
- [58] M. S. Abel, P. G. Siddheshwar, and M. M. Nandeppanavar, "Heat transfer in a viscoelastic boundary layer flow over a stretching sheet with viscous dissipation and non-uniform heat source," *Int. J. Heat Mass Transf.*, vol. 50, no. 5–6, pp. 960–966, Mar. 2007. DOI: [10.1016/j.ijheatmasstransfer.2006.08.010](https://doi.org/10.1016/j.ijheatmasstransfer.2006.08.010).